1979-12

Experimental study of self-scanning photodiode array.

Martins, Carlos J. G.

Monterey, California : Naval Postgraduate School

EXPERIMENTAL STUDY OF SELF-SCANNING PHOTODIODE ARRAY

Carlos J.G. Martins

NAVAL POSTGRADUATE SCHOOL
Monterey, California

THESIS

EXPERIMENTAL STUDY OF SELF-SCANNING
PHOTODIODE ARRAY

by

Carlos J. G. Martins

December 1979

Thesis Advisor: E. C. Crittenden, Jr.

SECURITY CLASSIFICATION OF THIS PAGE (When Data Entered)

REPORT DOCUMENTATION PAGE

READ INSTRUCTIONS BEFORE COMPLETING FORM

1. REPORT NUMBER	2. GOVT ACCESSION NO. / 3. RECIPIENT'S CATALOG NUMBER
4. TITLE (and Subtitle): Experimental Study of Self-Scanning Photodiode Array	5. TYPE OF REPORT & PERIOD COVERED: Master's Thesis December 1979
	6. PERFORMING ORG. REPORT NUMBER
7. AUTHOR(s): Carlos J. G. Martins	8. CONTRACT OR GRANT NUMBER(s)
9. PERFORMING ORGANIZATION NAME AND ADDRESS: Naval Postgraduate School Monterey, California 93940	10. PROGRAM ELEMENT, PROJECT, TASK AREA & WORK UNIT NUMBERS
11. CONTROLLING OFFICE NAME AND ADDRESS: Naval Postgraduate School Monterey, California 93940	12. REPORT DATE: December 1979 / 13. NUMBER OF PAGES: 60
14. MONITORING AGENCY NAME & ADDRESS(if different from Controlling Office): Naval Postgraduate School Monterey, California 93940	15. SECURITY CLASS. (of this report): Unclassified / 15a. DECLASSIFICATION/DOWNGRADING SCHEDULE

16. DISTRIBUTION STATEMENT (of this Report)

Approved for public release; distribution unlimited

17. DISTRIBUTION STATEMENT (of the abstract entered in Block 20, if different from Report)

18. SUPPLEMENTARY NOTES

19. KEY WORDS (Continue on reverse side if necessary and identify by block number)

ensors; Arrays; Photodiodes; Noise; Self-Scanning

20. ABSTRACT (Continue on reverse side if necessary and identify by block number)

An experimental study of a new series of Solid State image ensor arrays was conducted, operating in a photon flux integration ode. The operation of a P-N junction photodiode is analyzed, and oundary conditions to operate the device are presented. The rigin of the switching noise as the predominant noise source is erified. Some applications are developed.

FORM 1 JAN 73 1473 EDITION OF 1 NOV 65 IS OBSOLETE

Approved for public release; distribution unlimited

Experimental Study of Self-Scanning Photodiode Array

Carlos J. G. Martins
Lieutenant, Portuguese Navy

Submitted in partial fulfillment of the
requirements for the degree of

MASTER OF SCIENCE IN PHYSICS

from the

NAVAL POSTGRADUATE SCHOOL
December 1979

ABSTRACT

An experimental study of a new series of Solid State image sensor arrays was conducted, operating in a photon flux integration mode. The operation of a P-N junction photodiode is analyzed, and boundary conditions to operate the device are presented. The origin of the switching noise as the predominant noise source is verified. Some applications are developed.

TABLE OF CONTENTS

ACKNOWLEDGMENTS

I would like to acknowledge Professor E. C. Crittenden for his help, patience, and assistance in the preparation of this report. I would also like to thank him, as well as Professor A. Cooper who reviewed the final manuscript, and provided many helpful suggestions. Finally, having produced this report, I understand why other authors always thank their spouses. It is they who must put up with the greatest amount of hassle. Thank you dear wife, you are great!

I. INTRODUCTION

A. GENERAL

Advances in the fabrication of photosensitive elements and integrated circuits have led to significant progress in the development of self-scanned image sensors, which produce a video signal without the help of an electron beam. Such a system is shown in Figure 1.

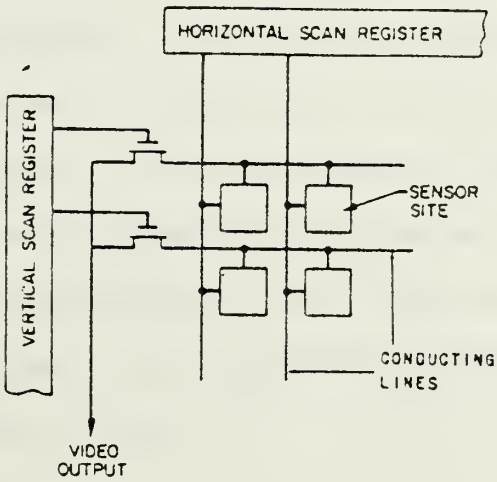

Figure 1

It consists of an array of photosensitive elements, each located at the intersection of mutually perpendicular address strips which are connected to scan generators and video coupling circuits. The application of sequential scan pulses to the address strips permits an image to be scanned and a video signal to be produced, similar to that generated by a television camera tube. To obtain image detail comparable to broadcast television, however, the array must contain thousands of picture elements. More recently other types of device have

appeared-C.C.D.'s - that perhaps in the future can replace camera tubes for most of the applications. Immediate applications of solid state line scanners are character-recognition optical readers for computers or aides for the blind.

In particular the device used in this research is well suited for optical character recognition (O.C.R.).

Although still exceeding camera tubes in cost, solid state sensors offer significant advantages which are of interest to potential users. Digital scanning provides a geometric accuracy of scan and a versatility of addressing not possible with electron beams. The much greater compactness of a self-scanned sensor can be important in certain applications. A natural expected reduction of cost and power consumption should introduce many new applications which have not been possible for camera tubes.

B. SUMMARY OF OPERATION

In the vidicon television camera, light from the scene is imaged onto a photoconductive layer which is scanned with an electron beam. The continuous photoconductive target (which functions as if it were a discrete array of P.C. elements) is contacted in sequence by the electron beam. In our solid state sensor the beam is replaced by a set of sequentially operated switches permanently connected to each photosensor element. The switches are transistors located at the picture elements, and are normally turned off, being activated

in sequence by means of pulses supplied by the scanning circuit. The device uses the charge storage mode; to permit integration of light for the entire period between scans an associated capacitor is used. It is clear that the charge storage mode is only possible if the RC time constant of the capacitor in series with its switch exceeds the integration time. The dark resistance of the photosensor and the off-resistance of the switch must therefore be very high. Figure 2 shows a simplified circuit of the device:

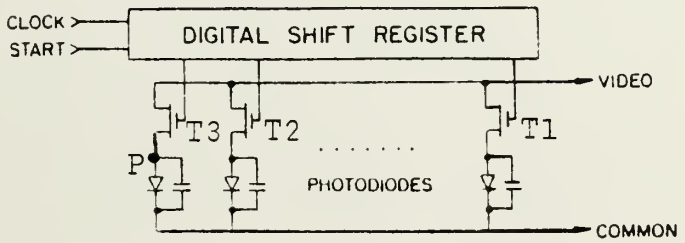

Figure 2

When light falls on the photoconductor, the capacitor is gradually discharged and point P rises in potential. The charge pulse which flows in the external circuit (video) during the sampling period is equal to the total charge which had leaked off the capacitor during the light integration period.

The effective signal current gain introduced by storage is given by:

$$G_c = \frac{T_L}{T_s}$$

where T_L is the integration period and T_s the sampling period. The photodiode is held in reverse bias at all times and the depletion-layer capacitance provides the storage.

The digital shift register in Figure 2 provides the sequence to operate the switches. The scanning pulse quickly reduces the potential at point P to ground, charging the capacitor.

II. DETAILED STUDY OF THE DEVICE

A. THE CHARGE STORAGE MODE

1. Array in the dark

We start by a study in the dark; that is, considering the array not illuminated. If the diode is charged and there is not illumination incident on the diode, the only current available to discharge the space-charge capacitance is the generation-recombination current in the space-charge region, given by:

$$I_{gr} = \frac{A\ q\ n_i}{2\ t_o} \tag{1}$$

with: A--Junction Area

q--Electronic Charge

W--Space-charge Width

n_i--Intrinsic Concentration

t_o--Effective Life-time

that yields:

$$I_{gr} = \frac{A\ q\ n_i}{2\ t_o} \left(\frac{12\ \varepsilon}{q\ a}\right)^{1/3} V^{-1/3} \tag{2}$$

with: a--Net Doping Gradient at the juntion

ε--Permittivity for silicon

The junction capacitance is a function of the applied voltage and is given by:

$$C(v) = A \left(\frac{q\ a\ \varepsilon^2}{12}\right)^{1/3} V^{-1/3} \qquad (3)$$

For an open-circuit junction, the generation-recombination current must equal the capacitive displacement current. The resulting current balance expression is:

$$C(v)\ \frac{dV(t)}{dt} = -\ I_{gr} \qquad (4)$$

Substituting the earlier relations into the above we have:

$$V^{-2/3}\ \frac{dV(t)}{dt} = \frac{-3\ n_i}{2\ t_o} \left(\frac{144\ q}{\varepsilon\ a^2}\right)^{1/3} \qquad (5)$$

Integrating and employing the boundary conditions that, at $T = 0$ the voltage across the junction is V_0 yields the expression for junction voltage as a function of time.

$$V(t) = \left(V_o^{1/3} - \frac{n_i}{6\ t_o} \left(\frac{144\ q}{\varepsilon\ a^2}\right)^{1/3} t\right)^3 \qquad (6)$$

This dark response imposes three limitations on the operating characteristics of the array: 1) Finite storage time; 2) Fixed pattern noise; 3) A temporal noise.

The length of time required for the dark current to discharge the space-charge capacitance can be calculated from (6) and is:

$$t_c = V_o^{1/3}\ \frac{6\ t_o}{n_i} \left(\frac{\varepsilon\ a^2}{144\ q}\right)^{1/3} \qquad (7)$$

The dark leakage current varies from element to element but is typically less than 1 pA at room temperature. For our device t_c = 3 sec. Then the dark current would contribute an output charge of .03 pCoul. with a scanning time t_o = 30 ms.

Since the saturation charge is 3 pCoul., dark current will contribute about 1% of the saturated output signal for t_o = 30 ms ; 0.1% for t_o = 3 ms and so on. The dark current is not completely uniform throughout the device. This effect imposes a fixed pattern noise on the signal, limiting the minimum signal that can be detected.

2. Illuminating the array

In this section we will consider the array illuminated; then the photocurrent adds to the diode dark current, causing a more rapid discharge of the junction capacitance. The current is given by:

$$I_p = I_o E \tag{8}$$

with: I_o--The Photosensitivity

E --The Irradiance

Following similar steps, as in the section before, the result is:

$$V(t) = \left(V_o^{2/3} - \frac{2}{3} I_o E A \left(\frac{12}{q a \varepsilon^2}\right)^{1/3} t\right)^{3/2} \tag{9}$$

3. The Sampling Time

In the previous sections, relations for the dark and video signal were found. Considering Figure 2, transistors T1

T2, T3 are simply the switches, that operate periodically. When they are closed, the junction capacitance is charged. As we are going to see later, a clock pulse turns ON and OFF the switches T1, T2,.....

The quantity of charge that flows through the output circuit during t_s is proportional to the incident photon flux integrated over the scan time t_o. With the output of the diode sampled periodically, a quantity of charge Q_c is given by:

$$Q_c = I_p \, t_s \tag{10}$$

Since the diode is operating in the charge storage mode, the charge Q_s that flows through the output circuit during the sample time t_s is the sum of the charge generated during the scan time plus the charge Q_c generated during the sample time, that is:

$$Q_s = (t_L - t_s) \, I_p + t_s \, I_p = t_L \, I_p \tag{11}$$

with t_L the integration time. Our device has a fixed sample time of 500 ns corresponding to the width of the clock pulse. During the sample time it is desirable to recharge the diode as completely as possible. The relation giving the sample time, in terms of the final voltage as a function of the operating parameters, is:

$$t_s = \frac{R_L C_{Vo}}{2} \left(\frac{\pi}{\sqrt{3}}\right) \ln F\left(\frac{V_2}{V_o}\right) - 2\sqrt{3} \tan^{-1} G\left(\frac{V_2}{V_o}\right)$$

with: $$G\left(\frac{V_2}{V_o}\right) = 2/\sqrt{3} \left(\left(\frac{V_2}{V_o}\right)^{1/3} + \frac{1}{2}\right)$$

$$F\left(\frac{V_2}{V_o}\right) = \frac{(V_2/V_o)^{2/3} + (V_2/V_o)^{1/3} + 1}{(V_2/V_o)^{2/3} - 2(V_2/V_o)^{1/3} + 1}$$

Figure 3 represents a plot of the relation above. It shows the dependence of the ratio of the final voltage on the junction to the supply voltage, as a function of the sample time t_s . A trade-off exists in the choice of the sampling time: a small sampling time allows a greater gain, but also a small sampling time may not allow the necessary charge of the diode. The value of 500 ns in our device is a very good one. The ratio of $V_2/V_o = 1$. The manufacturer's sheet also recommends a minimum value of 20 ns if an external clock is desired. This is a reasonable value, but nevertheless a little low, since $V_2/V_o = .962$. By our results any value of t_s lower than 100 ns should not be used.

4. The Scanning Time

We have seen that some limitations exist with respect to the sample time. Now we are going to see what limitations we have with respect to the scan time. Neglecting the product $I_p R_L$ it is found that:

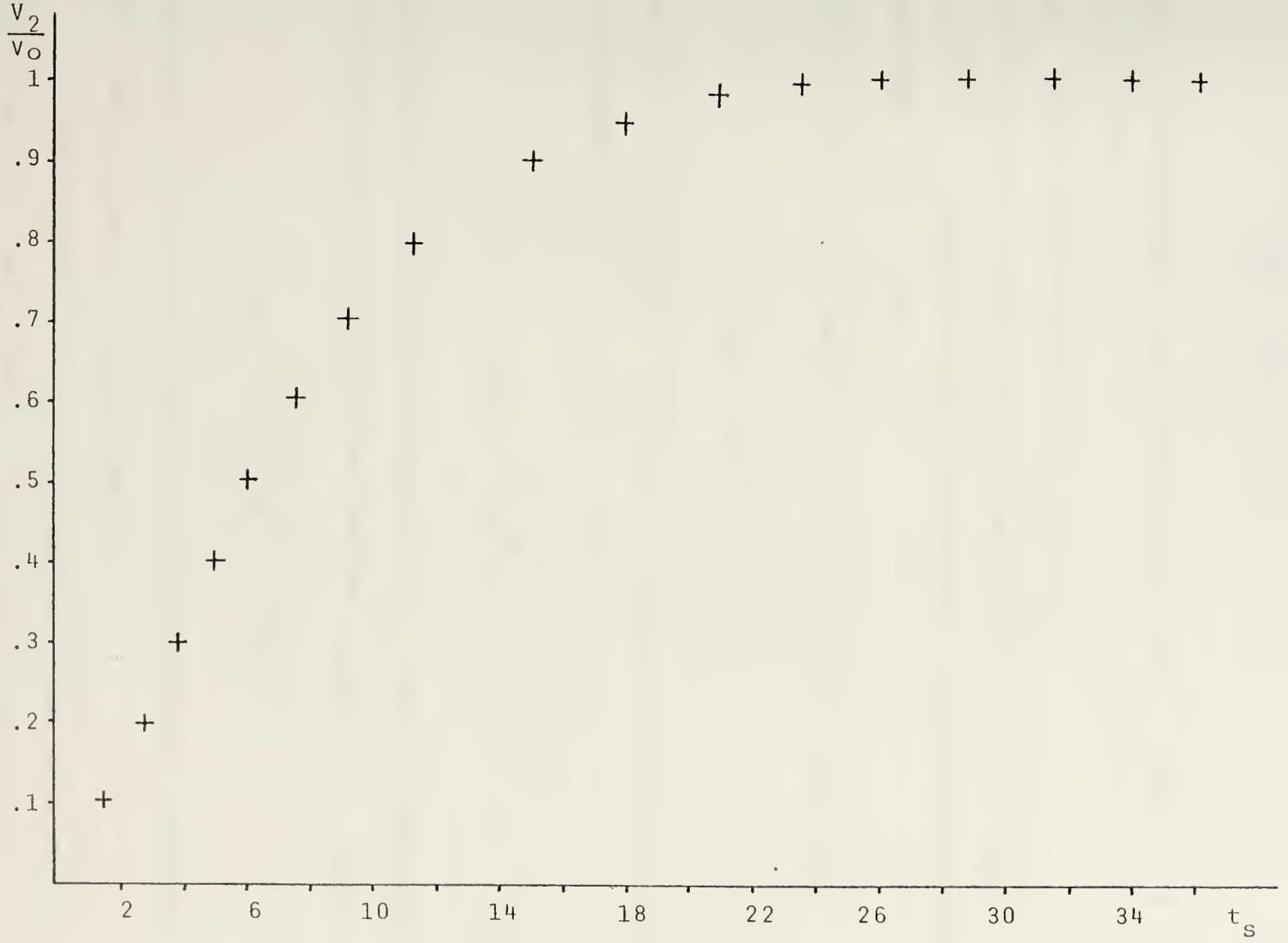

Figure 3

$$\frac{Q_{SM}}{Q_{MI}} = \frac{I_p\ (t_o + t_s)}{\frac{3}{2}\ C_{Vo}\ V_o} = (V_2/V_o)^{2/3} \qquad (12)$$

Q_{SM} is the maximum signal charge which may be read for a given value of V_2 .

Q_{MI} is the signal charge when $V_2 = V_o$.

As we have seen in the previous section, the sample time is of sufficient duration to fully recharge the junction capacitance, and then $\frac{Q_{SM}}{Q_{MI}}$ is one.

Then we can find an expression for the maximum scan time:

$$t_{o/Max} = Q_{MI}\left(\frac{\dot{1}}{I_o\ E + I_{gr}}\right) \qquad (13)$$

Defining, for practical purposes, a minimum illumination level as one where $I_p = 10\ I_{gr}(V_o)$, then:

$$E_{/Min} = \frac{10\ I_{gr}}{I_o}\ V_o \qquad (14)$$

Considering the generation-recombination current independent of voltage and evaluated at the maximum voltage V_o , then:

$$E_{/Min} = \frac{10\ q\ n_i\ V_o^{1/3}}{2\ t_o\ I_o}\left(\frac{12\ \varepsilon}{q\ a}\right)^{1/3} \qquad (15)$$

Relations (13) and (15) define the conditions for the storage mode operation at low light levels.

Limitations at high illumination levels also require investigation. The following relation can be derived:

$$\frac{Q_{SM}}{Q_{MI}} = \left(\frac{I_p \ R_L}{V_o} - 1 \right)^{2/3} \qquad (16)$$

The effect of the current generated during the sample time is to reduce the initial charge on the junction capacitance and cause an uncertainty in the output signal.

Assuming $I_p \ R_L \leq .01$ then:

$$E_{/Max} = \frac{.01 \ V_o}{I_o \ R_L} \qquad (17)$$

From relation 13 the scan time required to fully discharge the diode, assuming I_{gr} small compared with the, generated, photocurrent is:

$$t_{o/Max} = \frac{Q_{MI}}{I_o E} = \frac{1,28 \ X \ 10^{-6}}{E} \quad \text{sec} \qquad (18)$$

with Q_{MI} the saturation charge = $3.2 \ X \ 10^{-12}$ Coul.

$$I_o = 2.5 \ X \ 10^{-6} \ A/W/cm^2 \qquad (18)$$

The value of the minimum detectable illumination, considering the worst case, $I_{gr} = 1 \ X \ 10^{-12}$ A , is given by equation (14)

$$E_{/Min} = 2 \ X \ 10^{-5} \ W/cm^2$$

At this illumination level the maximum scanning time is:

$$t_{o/Max} = \frac{1.28 \ X \ 10^{-6}}{2 \ X \ 10^{-5}} = 64 \ ms$$

The limitation at high illumination level is obtained from (17):

$$E_{/Max} = 4 \text{ W/cm}^2$$

Since the maximum scan time becomes very short a duty factor (t_o/t_s) must be considered:

$$t_{o/Max} = \frac{3.2 \times 10^{-7}}{1 + \frac{t_o}{500 \times 10^{-9}}} = .22 \text{ µs}$$

We must note that these are theoretical values and that in practice there is a sensible difference. Experimental values were obtained and will be presented in a later section.

B. DETAILED OPERATION

Figure 4 represents the device in a more complete way. We can see that is composed of two distinct parts:

1. - Dummy and photodiodes
2. - Shift register scanning circuit

These will be discussed in the next sections.

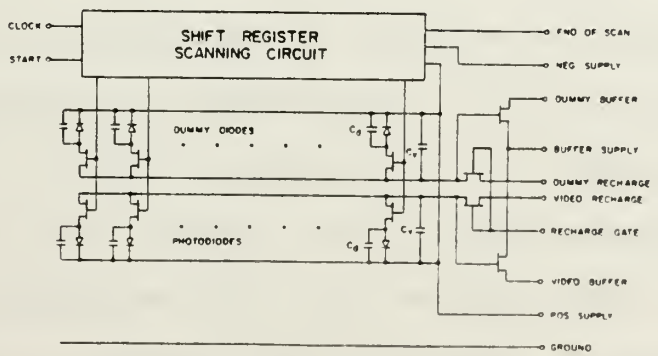

Figure 4

1. Dummy and Photodiodes

In this section the origin of the transients and how the use of Dummy diodes increases the performance of the circuit will be discussed. Figure 5 represents an elementary cell

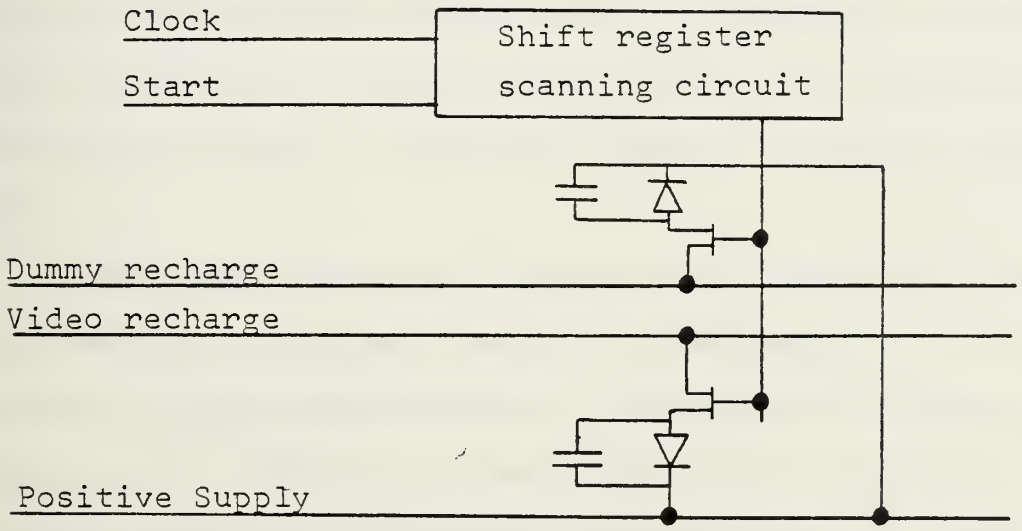

Figure 5

The noise which is due to capacitive coupling of interrogating pulses to the output of the sensor constitutes a limitation on the performance of the device. Transistors T1, T2 are OFF during the integration period and ON during the short clock period, corresponding to the time of discharging and charging the capacitor respectively. When a given element is interrogated, a pulse is applied to each transistor. Displacement currents flow, through the initially reverse-biased junction of the photodiode until the voltage across the junction is sufficient to forward bias the diode. In addition to this transient a displacement current flows through each of the

shunt capacitances of the remaining reverse-biased diodes in the array, causing a positive voltage spike to appear at the output.

At the termination of the sampling pulse the coupling capacitors share their charge with the photodiode and additional displacement current flows through the remaining reverse-biased diodes in the array causing a negative voltage spike.

The same reasoning applies to the remaining elements in the array. In summary, switching corresponds to a change of state and this corresponds to introducing transients in the output signal. We can now see how our device decreases these unwanted switching waveforms by using two rows of diodes, of which only one is light sensitive.

When the clock signal arrives, it switches both T1 and T2 (Dummy and Photodiodes), and since the circuits are identical, the same transient response appears for both circuits. From the dummy circuit the only response is a transient waveform. From the photocircuit (video line) the response is a composite signal: one component caused by the light and another caused by the transient signal. Since the two circuits are identical and we know the transient signal we subtract the two signals. A schematic diagram of this operation is given in Figure 6.

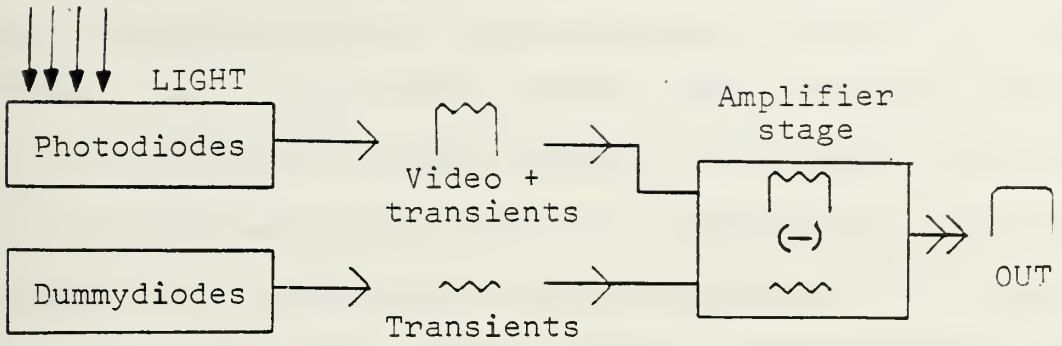

Figure 6

All this seems easy to accomplish but in practice it does not function very well, simply because the transient signals are not equal. Capacitor noises result from mismatches between parasitic gate-source and gate-drain MOS capacitances, and then some variation in amplitude of the spikes exists. That variation in amplitude throughout the MOS photoarray gives rise to a fixed pattern noise in the video pass-band-noise that cannot be filtered. Fortunately the variation in the amplitude is small compared with the absolute amplitude.

2. Shift Register Scanning Circuit

It consists of two, two-phase, dynamic shift registers and a drive circuit. It allows sequential interrogation (scan) of the array using two video lines. The ODD sixty-four diodes are multiplexed to one of the video lines and the EVEN sixty-four are multiplexed to the other video line.

Let us see how this readout is processed. The MOSFET switch, discussed before, is activated and connects the common video line to one of the diodes. When switching takes place, the charge is suddenly dumped on the common video line, which is connected to the input of a preamplifier. The switching MOSFETS are sequenced by a pair of digital shift registers. At the beginning of the scanning cycle, a digital ONE is introduced onto the first element of the shift register. Every clock pulse makes this digital ONE propagate one element further. The presence of the ONE turns on the adjacent MOSFET switch, discharging the diode. The operation of the two-phase shift register is presented in the next section.

3. The Two-phase Dynamic Shift Register

The two-phase dynamic shift register is constructed by cascading two dynamic MOS inverters (Figure 7).

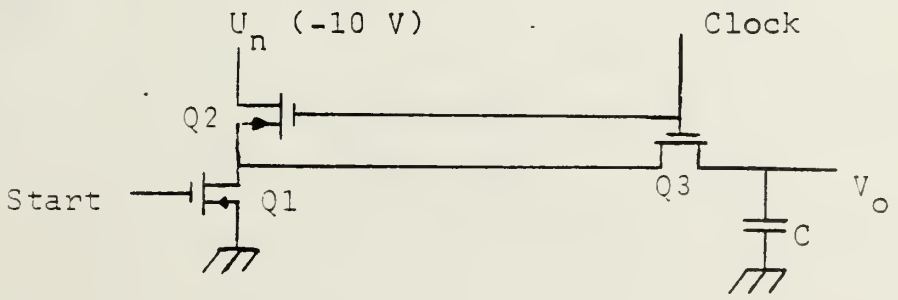

Figure 7

The circuit of Figure 7 requires the clock waveform for operating. The capacitor C represents the parasitic ca-

pacitance between the gate and substrate of the following MOS, fed by U_o . When ϕ = 0 volts, the gates of Q2, Q3 are at 0 volts and both these enhancement MOS are OFF. The supply voltage is disconnected from the circuit and delivers essentially no power. When the clock is at -10 volts, Q2, Q3 are ON and inversion of U_i takes place. Cascading two circuits as shown in Figure 7, the information stored in capacitance C is transferred to the following inverter by applying a second clock pulse out of phase with the first waveform. Figure 8 represents the two-phase dynamic shift register for one element.

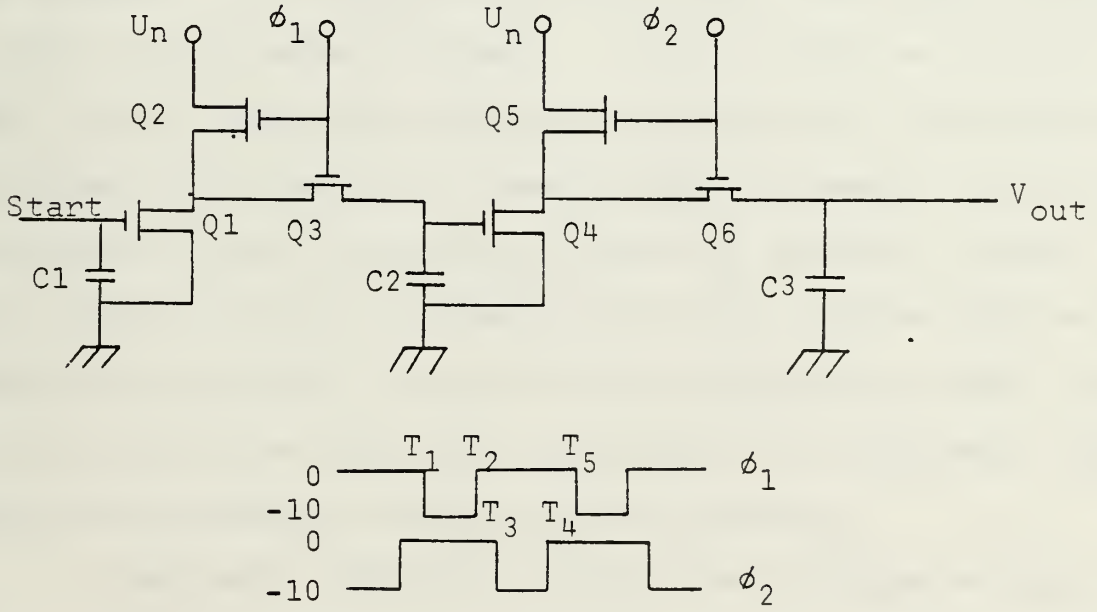

Figure 8

The start pulse is the voltage at the capacitor C1.

i-- When ϕ = - 10 volts at $t = t_1$, Q1 and 02 form an

inverter and Q3 conducts. Then the complement of the start pulse is transferred to C2.

ii- When ϕ = 0 volts at $t = t_2$, Q2 and Q3 are OFF and C2 retains its charge.

iii- When ϕ = - 10 volts at $t = t_3$, Q4 and Q5 act as an inverter and Q6 is closed. Then the voltage stored at C2 is again inverted and stored at C3. Then at C3 we simply have the start pulse again, but delayed by an amount determined by the clock period. This delayed start pulse acts in the transistor switches and allows the readout of the sensor element. It is important to note that the circuit before is only for one sensor element. If we cascade two circuits, like the one, the start pulse is delayed by two clock periods and allows the readout of a second sensor element. It is interesting to note that since we have 128 elements, we have the circuit of Figure 8 repeated 128 times. Since each has 6 transistors we have a total of 768 transistors in about 3 mm^2. In our device there are two, two-phase shift registers, each one with 64 elements for odd and even sensors.

The numder 768 above, is important because we can consider the 768 transistors to be practically in series, affecting the speed of response of the device.

4. <u>The Speed of Response</u>

There are two intrinsic limits on the speed of response:

i- A basic limit set by the time for charge transport along the channel-TRANSIT TIME LIMITATION. The MOS is normally a closed switch, then biased into the saturated region of operation. The transit time is given by:

$$T_{tr} = \frac{4}{3} \frac{L^2}{u_n (V_G - V_T)}$$

Considering typical values for our device, $T_{tr} = 4.4 \times 10^{-10}$ sec.

ii- A limit imposed by the charging of capacitances that are inherent in the device structure. Several capacitances exist, but only one is essential for the operation of the transistor. This is the capacitance between the gate and the channel, that controls the conductance between the drain and the source. The others result from the device structure. Reducing their size improves the switching speed. The typical time to charge C_{gs} is about 4×10^{-9} sec. This value is about 10 times the value found before. Returning to Figure 8 we see that Q1 and Q2 determines the speed of response of the array, since the capacitance C_{gs} must be charged during a portion of the cycle. An approximate value of the speed of response can then be calculated to be about .5 μsec.

III. EXPERIMENTAL STUDY

A. THE START AND CLOCK PULSES

We know from the study before, that each time the start pulse goes high the first element in the array begins to be read. We also know that each time the clock pulse goes high an element is read. Then, as a result, we have to provide a time between two start pulses of:

$$T_L = 128 \text{ X } T_{clock}$$

The number of elements of the array is 128, (denoted by N), and is set by the counters in the circuit. These three counters allow a combination from 1 to 4095 and the clock frequency adjustment allows a frequency range from 80 KHz to 1 MHz. Since the time between start pulses is just the integration time, we have for this device a range of .13 ms to 51.2 ms for the integration time, assuming $N \geq 127$. Then a relation for the integration time is:

$$T_L = N \text{ X } T_{clock} \tag{19}$$

with: T_L--The integration time

N --The number of elements set in the counter

T_{clock}--The clock period

We will see later that several factors limit this range to a smaller one.

Figure 9 shows the clock waveform (above) and the start output (below) for an integration time of $T_L = 9\ T_{clock}$.

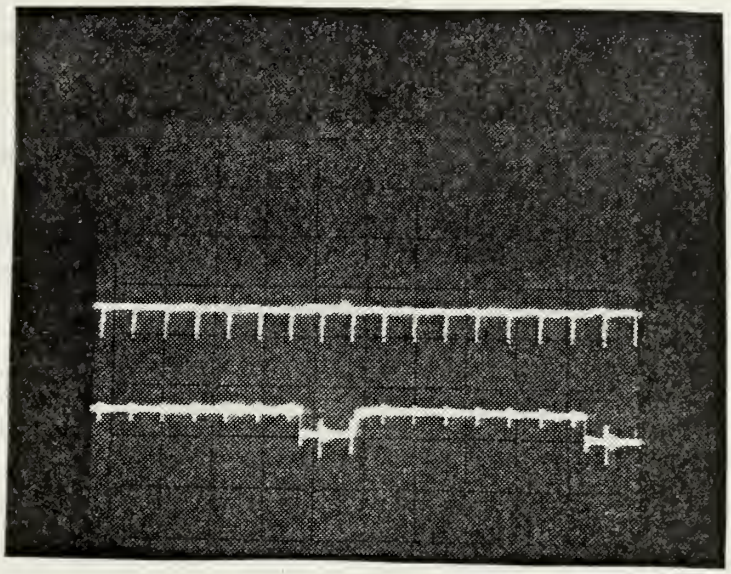

Figure 9

B. THE START AND VIDEO PULSES

From relation (19) we can see that for most of the integration times there are several ways to get the same integration time. For example, supposing that an integration time T_L = 1 ms was desired we can have two situations:

i -

T_L = 1 ms This can be achieved with N = 127

and $T_{clock} = 7.812 \times 10^{-6}$ sec.

ii -

T_L = 1 ms That can also be achieved with N = 700

and $T_{clock} = 1.429 \times 10^{-6}$ sec.

Clearly an infinite number of possibilities exist to achieve the same integration time. However from our earlier study we know that this doesn't make any difference in the performance

of the array, since the sample time and also the scanning time are the same. The two examples before can be used to get some indepth information about the array operation.

For the first process the situation is described in Figure 10 below:

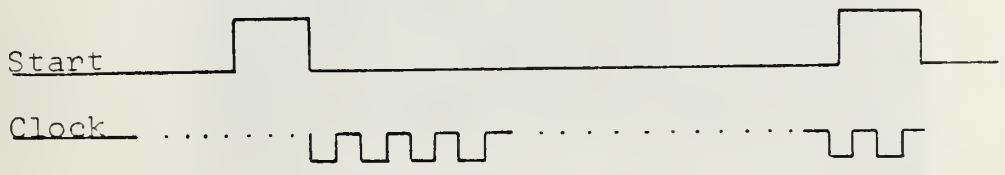

Figure 10

We set N = 127 meaning that 128 elements are going to be read. Then after reading the 128 elements a new start pulse appears, and the first element is read again. The video output is shown in Figures 11 and 12 for two different settings of the array. It must have 129 peaks. At Figure 12 we see the same output, with a first reading, followed by a complete second reading and a beginning of a third reading. The waveform in the top of this figure is the start pulse. We see that, after the last element of the first reading is read, the start pulse appears and a new reading begins.

For the second process we set N = 700 meaning that the counter is going to count until 700. But since our array only has 128 elements a time must appear without any output. There are 700-128 = 572 elements that don't exist and cannot give

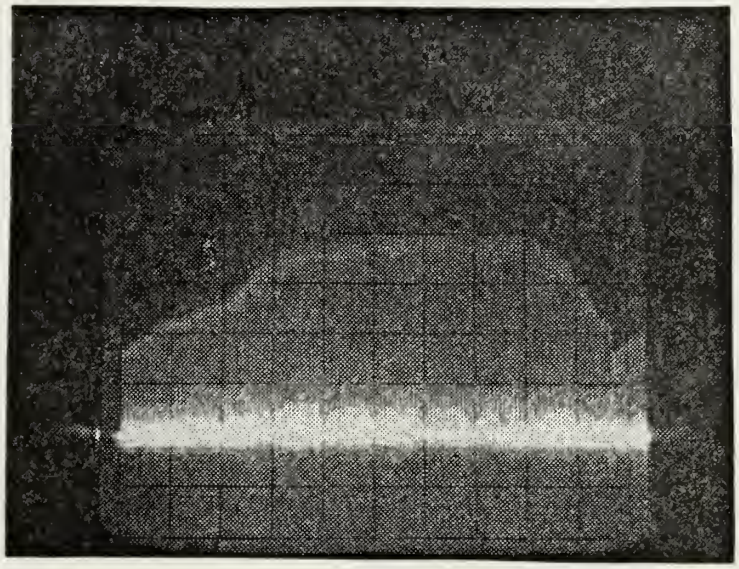

Figure 11

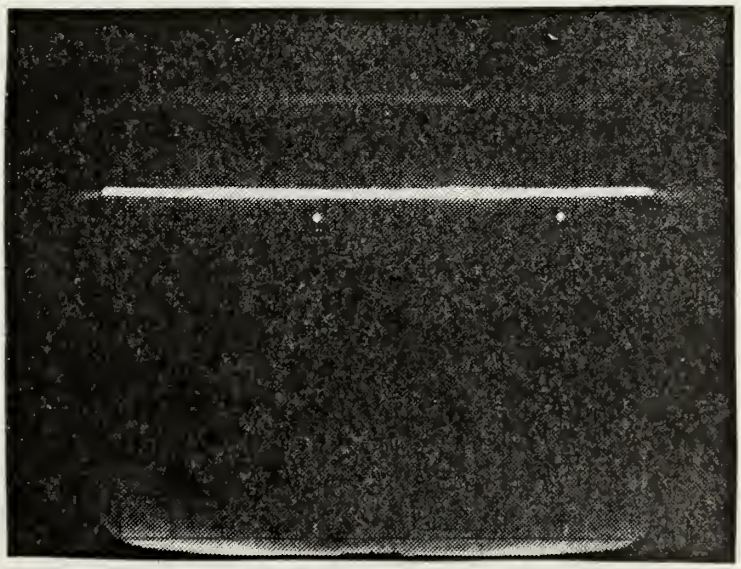

Figure 12

any output. This can be seen in Figures 13 and 14. These correspond to Figures 11 and 12 in the process before. The reasoning then presented applies in the same way to this second case.

At Figure 14 we see six readings of the array with the corresponding gaps at the output. An advantage of these gaps is that we can use them, simply adding more sensor chips in series, using the same electrical circuit. Also from the figures before, we see we have, for both processes, the same output voltage as was expected.

C. COMPARISON OF THEORETICAL AND EXPERIMENTAL VALUES

Some theoretical values from previous sections, are useful to remember now:

i-- $E_{/Min} = 2 \times 10^{-5}$ W/cm^2 for $T_{L/Max} = 64$ ms

ii-- $E_{/Max} = 4$ W/cm^2 for $T_{L/Max} = .22$ μs

We noted then, that these were theoretical values and that in practice there were some differences, that we can see now. Corresponding to $T_L = 64$ ms our device can give us a maximum $T_L = 51.2$ ms .
Corresponding to $T_L = .22$ μs our device only gives us a $T_L = .13$ ms (a big difference). Then using these two new values for T_L we can recalculate, using the same relations as before and analogous steps, new values for $E_{/min}$ and $E_{/Max}$.

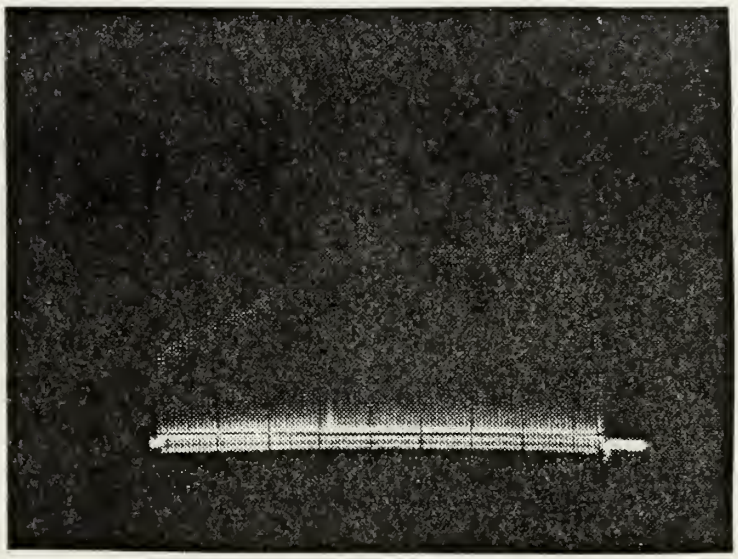

Figure 13

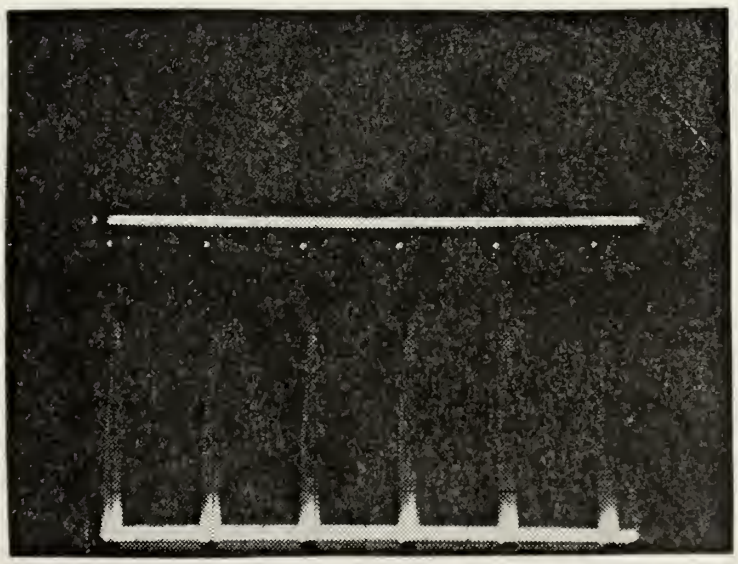

Figure 14

For T_L = 51.2 ms we have $E_{/min} = 2.5 \times 10^{-5}$ W/cm^2

For T_L = .13 ms we have $E_{/Max} = 9.85 \times 10^{-3}$ W/cm^2

The Manufacturer's sheet indicates a value for exposure- He - of: $He = 1.3 \times 10^{-6}$ Joules/cm^2 .

It is then interesting to check how our results before agree with this value.

The exposure is defined by:

$$He = E \times T_L$$

For T_L = .13 ms and $E = 9.85 \times 10^{-3}$ W/cm^2 we get for He :

$$He = 1.28 \times 10^{-6} \text{ Joules/cm}^2$$

in a complete agreement with the manufacturer's value.

For T_L = 51.2 ms and $E = 2.5 \times 10^{-5}$ W/cm^2 we get for He :

$$He = 1.28 \times 10^{-6} \text{ Joules/cm}^2$$

again in agreement with the manufacturer's value of 1.3×10^{-6} .

In order to complete this discussion it is only necessary to verify if this agreement still exists in the laboratory.

For this experimental determination of the minimum and maximum values of E we set N = 127 and the clock frequency to 1 MHz . Then the integration time was T_L = .13 ms . Using a P.I.N. photodiode as the calibrated detector, several readings were taken. The result is presented in Figure 15.

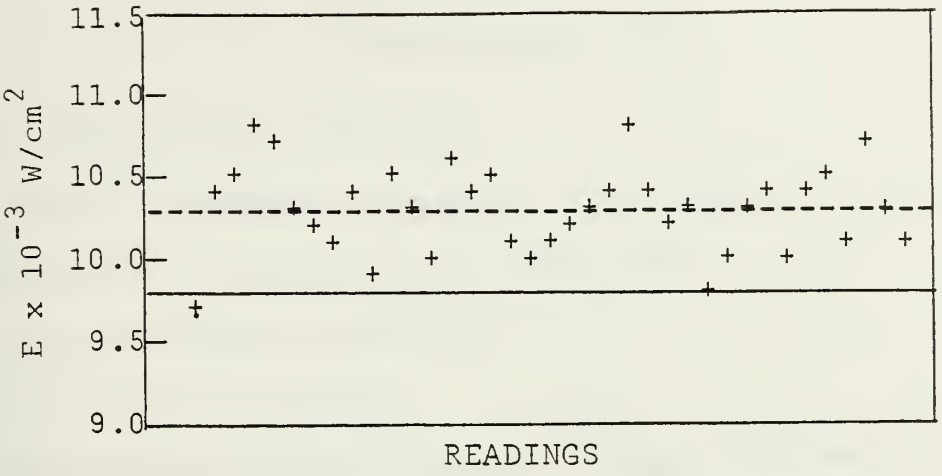

Figure 15

The line represents the theoretical and manufacturer's value. The crosses (+) are the experimental values, and the dashed line represents its approximate average. As we can see our experiment gives us an approximate value of $E = 10.4 \times 10^{-3}$ $W.cm^2$. There is then a small difference, perhaps due to non-calibration of the test detector. In a similar way the value of $E_{/min}$ can be checked. This situation is more difficult to evaluate due to the shape of the output signal in the oscilloscope. The experiment referred to in Figure 15 was conducted in the following way: For each point the source was placed in a position so as to have the device saturated. Afterward, the illumination was decreased slowly, until the output began to became unsaturated. At this point the irradiance was measured. The process was repeated for each reading.

IV. THE AMPLIFIER STAGE

A. THE DIFFERENTIAL AMPLIFIER

Figure 16 presents a diagram of the amplifier stage used in the circuit. It consists of two parts:

i--A Difference Amplifier

ii- A Video Amplifier

The existence of two signals - video and dummy - was explained before, as well as the necessity to subtract the dummy signal from the video. This operation is performed by the differential amplifier (DIFF. AMPL.). Figure 17 represents a linear active device with the two inputs video-Vi- and dummy-Du- and one output signal Vout. In an ideal DIFF-AMPL, we have:

$$V_{out} = A_d(Vi - Du) \qquad (20)$$

with: A_d - the gain of the differential amplifier

Vi - The composite video + transients

Du - The transients

In practice relation (2) is not applicable since the output also depends of the average level (Common-mode signal). Then we have:

$$v_d = Vi - Du \qquad \text{and} \qquad v_c = \frac{1}{2}(Vi - Du)$$

with: v_d - The Difference signal

v_c - The Common-mode signal

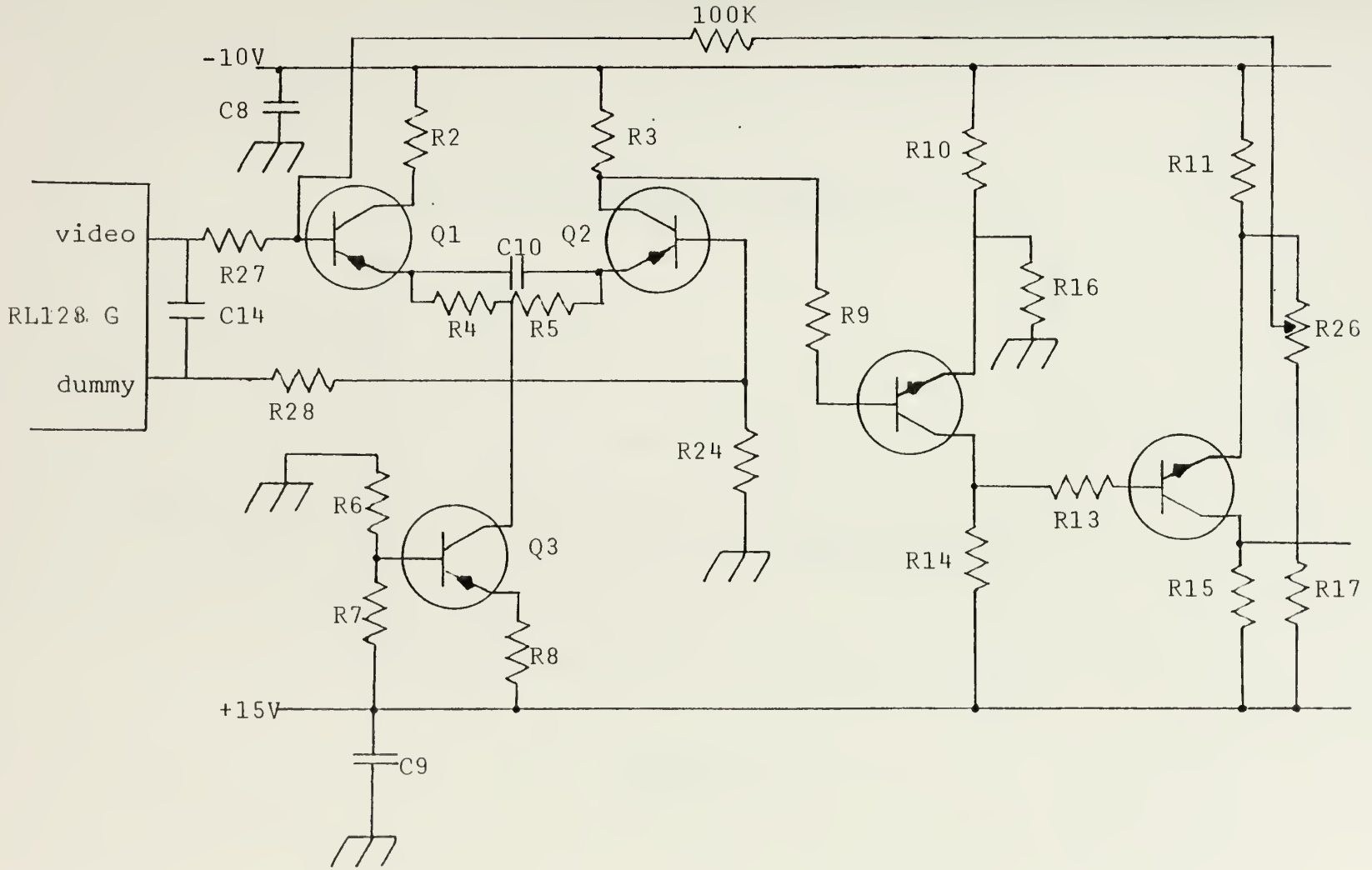
100K
-10V
C8
R2
R3
R10
R11
video
R27
Q1
C10
Q2
RL128. G
C14
R4
R5
R16
R9
R26
dummy
R28
R24
R6
Q3
R13
R14
R15
R17
R7
R8
+15V
C9

Figure 16

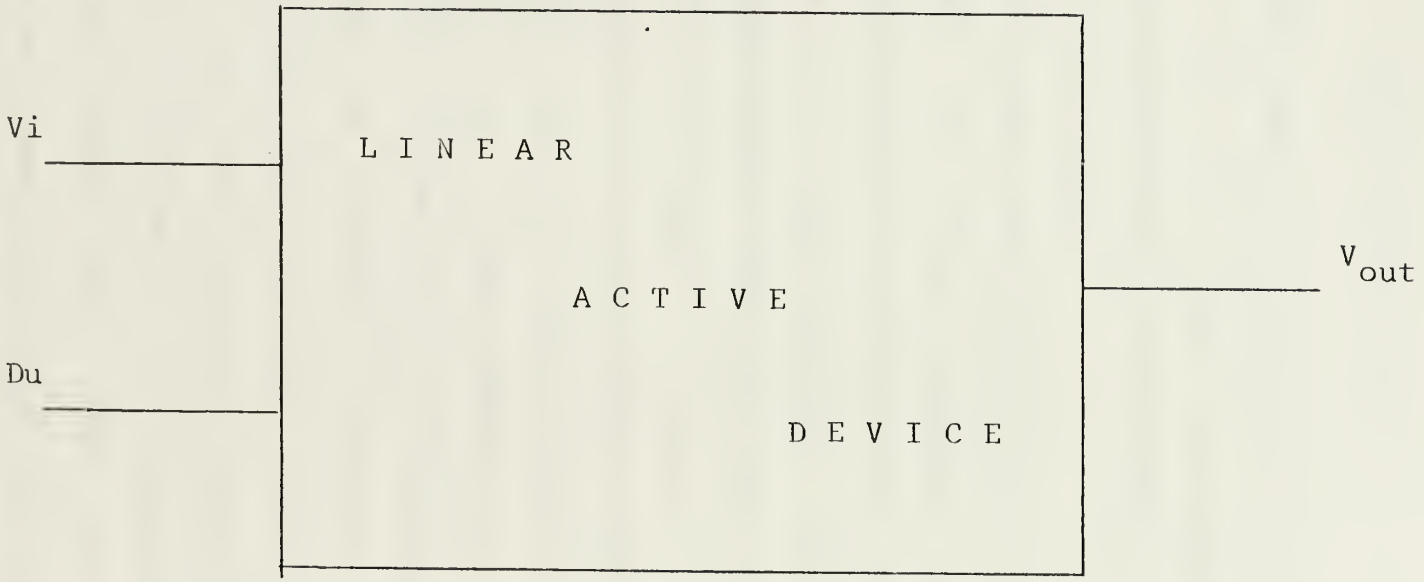

Figure 17

Then we have:

$$V_{out} = A_d V_d = A_c V_c \qquad (21)$$

The Diff-Ampl. used in the circuit is supplied with a constant current. Q1 , Q2 provide the common-mode rejection and amplify the remaining part of the signal. Q3 has a special function in the circuit.

An analysis of the circuit shows that, for Q1 and Q2 to operate properly, the emitter resistance has to be very large. The use of a simple resistance has limitations because of quiescent DC voltages across it. The emitter supply V_E = +15 volts must become larger for large values of R_e , in order to maintain the quiescent current at its proper value. If the operating currents of the transistors are allowed to decrease, this will lead to higher values of h_{ie} and lower values of h_{fe} . These decrease the common-mode rejection. Q3 has just the function of emitter resistance, with R6 , R7 and R8 adjusted to suitable values to give the necessary quiescent conditions for Q1 and Q2 . The circuit has then a very high effective resistance. Q3 really acts as a constant current source with the condition that the base current of Q3 is very small. Then, with all the conditions above, we have the circuit with the common-mode gain equal zero (gain of the signals common to the video and dummy). These are simply the transients that we want to eliminate.

B. PRACTICAL RESULTS AND CONSIDERATIONS

We already know that the output of the device is not zero for illumination. One of the reasons is the dark current. However the amplifier also has its role in the process. A question arises at this point. Is the amplifier unable to completely reject the common signal - transients - or is the array the cause of the problem of unequal signals in the dummy and video lines? Figure 18 gives the pin configuration for our array. In order to answer the question, the video line at pin 7 was disconnected, and instead, the dummy line was connected. Then it was possible to have at the input of the amplifier two absolutely equal signals.

Then we have:

$$v_d = 0 \quad \text{and from 21}$$

$$V_{out} = A_c V_c \quad \text{with} \quad V_c = 2V_i$$

The theoretical result of V_{out} should be zero, since for the Diff. Ampl. A_c is also zero.

The common-difference gain A_d can also be obtained, by using two equal signals with one inverted in respect to the other. Since we are more interested in the common-mode, this possibility was not evaluated.

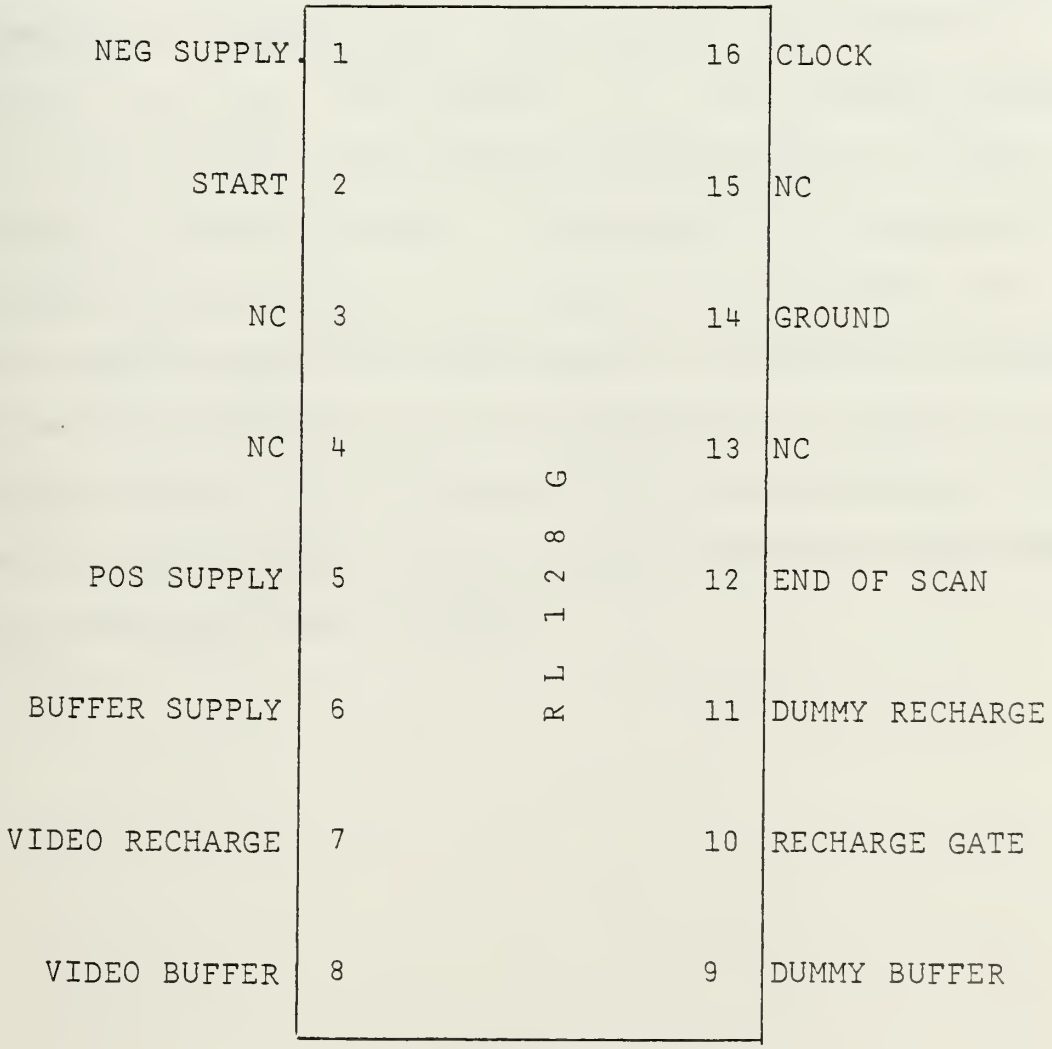
NEG SUPPLY
1
START
2
NC
3
NC
4
POS SUPPLY
5
BUFFER SUPPLY
6
VIDEO RECHARGE
7
VIDEO BUFFER
8
RL128G
16
CLOCK
15
NC
14
GROUND
13
NC
12
END OF SCAN
11
DUMMY RECHARGE
10
RECHARGE GATE
9
DUMMY BUFFER

Figure 18

Some considerations must be made about this circuit.

i- The use of single transistors is not the best way in this kind of circuit. Drift due to variations of h_{FE} V_{BE} and I_{CBO} with temperature is relevant. The circuit only operates correctly if the current I_o in Figure 16 is independent of temperature. For a typical dependence of 2.5 $mV/^oC$ of V_{BE3}, the current I_o is no longer constant.

ii- In addition, the matching of the devices is very important in these circuits. A good way is to construct the amplifier in an IC chip. Our circuit is constructed with single elements and with large physical separations between them, so it is possible for the temperature to change in individual elements. In IC chips, due to the proximity of the elements, any parameter changes due to temperature and power-supply variations tend to cancel.

V. SOME ASPECTS OF NOISE IN THE DEVICE

Noise introduced into the video signal by the image sensors and associated circuitry is probably the greatest factor that limits operation at low light levels.

The three main components for the dark output signal are:

1) The integrated dark leakage current

2) The fixed pattern noise, caused by incomplete cancellation of clock switching transients capacitively coupled into the video line.

3) Amplifier noise

A. THE DARK RESPONSE

The diode leakage current flows even in the dark. This aspect has been seen before. It appears as a DC background in the display. A plot of noise due to the dark leakage current is given in Figure 19, for a temperature of 25°C.

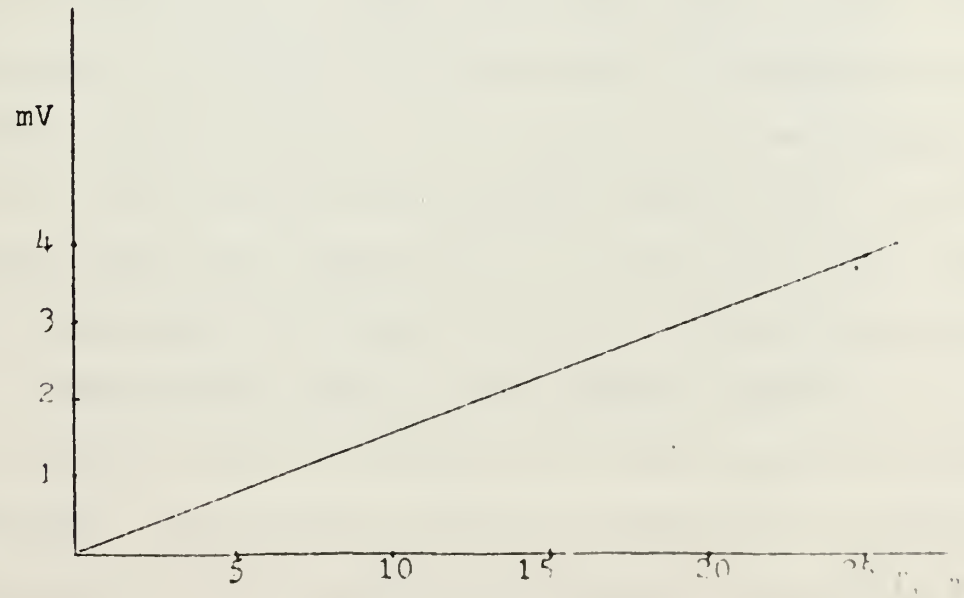

Figure 19

Figures 20 and 21 show two aspects of the dark response of our array. Each one corresponds to the two processes presented in section B of chapter III. We also must note that these two figures represent the sum of the three kinds of noise presented before.

1. Effect of the Two Rows of Diodes

Disconnecting pin 11 from the circuit, Figure 18, it was possible to evaluate the device with only the video line, for zero illumination. The result was that the noise increased by a factor of two compared with Figures 20 and 21. Then we must say that this design is really effective in reducing the noise in the array. Note that disconnection of pin 11 corresponds to operation of the array with only one row of diodes.

2. The Dark Response Components

We saw above that the switching noise is decreased using the differential readout. But we also see from Figure 22 or 23 that a noise signal with amplitude of about .07 V. still exists. Which of the components is predominant is an important point. Referring to Figure 19 we can accept a value of 2 mV for the dark leakage current noise. The noise component due to the amplifier is not also the main component of the noise seen in Figures 20 and 21. These figures present a fixed pattern noise in the display; however, the noise due to the amplifier is essentially a non-repetitive waveform fluctuation. Also typical values of the noise for these amplifiers are .1% of the saturation level, then about 4 mV .

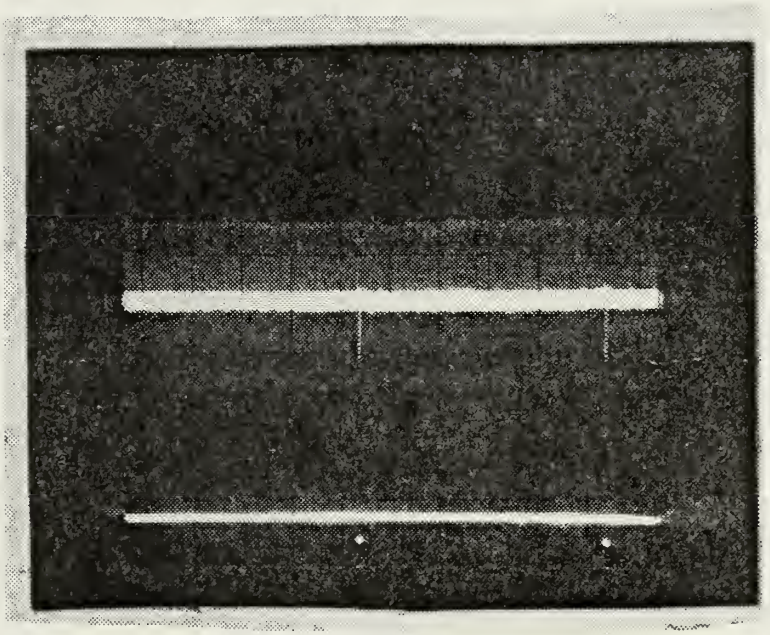

Figure 20

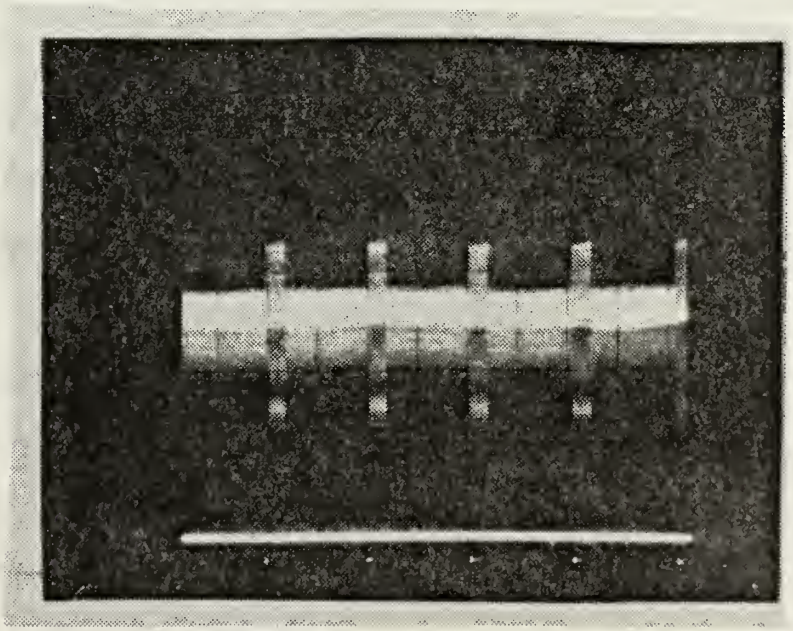

Figure 21

Finally we have the transient noise caused by the switching during the transfer process. From the two values above we see that this is really the problem. The switching transients govern the noise of the device, with an approximate amplitude of 40 mV . It is important to note that this is only true for small integration periods, since the dark leakage current has a linear dependence on the integration time. For larger integration times it becomes the principal source of noise. This is perhaps one of the most important results of this study since this is the point where some controversy exists between MOS solid state scanners and C.C.D.'s. It is claimed that, due to a different structure, the latter do not present this kind of noise.

To summarize, we have seen that the switching that takes place in reading the array gives rise to a noise signal that is predominant in most of the useful range of the device. Figure 22 summarizes these results. Note that, for an integration time of T_L = 30 ms , the dark current noise is approximately equal to the switching noise.

3. Device Uniformity

This is also an important parameter because a sensible nonuniformity through the array may cause misreadings and wrong intepretation of the output video.

In order to verify the response uniformity the following arrangement was set: A very small focused light spot was

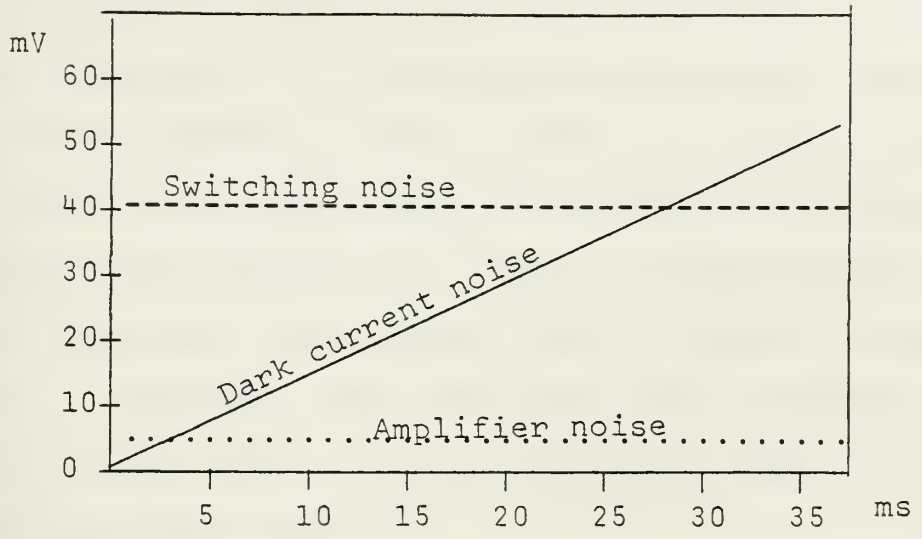

Figure 22

imaged on the first cell of the array, and the output recorded. The spot was then moved slowly along the array with the output recorded during this translation. The result is given in Figure 23 below.

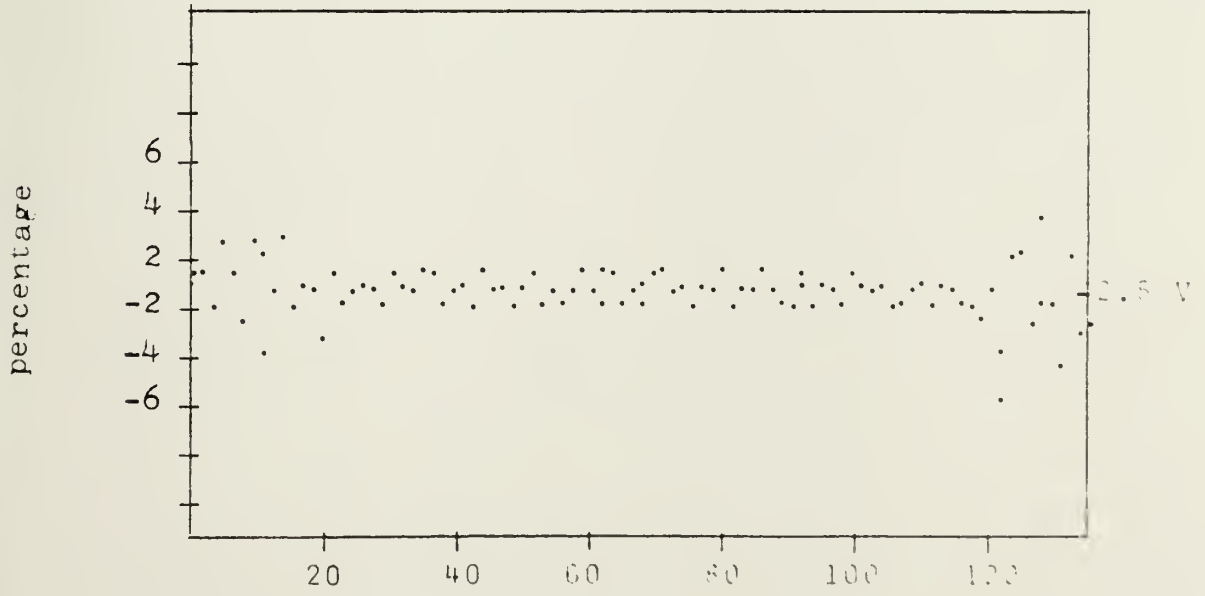

Figure 23

From this figure we see that the array has a good uniform response. However it is interesting to note that the larger values of nonuniformity appear at each end of the array.

Using the several results found earlier, a graph has been constructed (Figure 24). This is a useful graph, to be consulted when using the device, since it allows for each situation to determine the boundaries values governing the operation of the array. It also summarizes some of the results obtained in earlier sections.

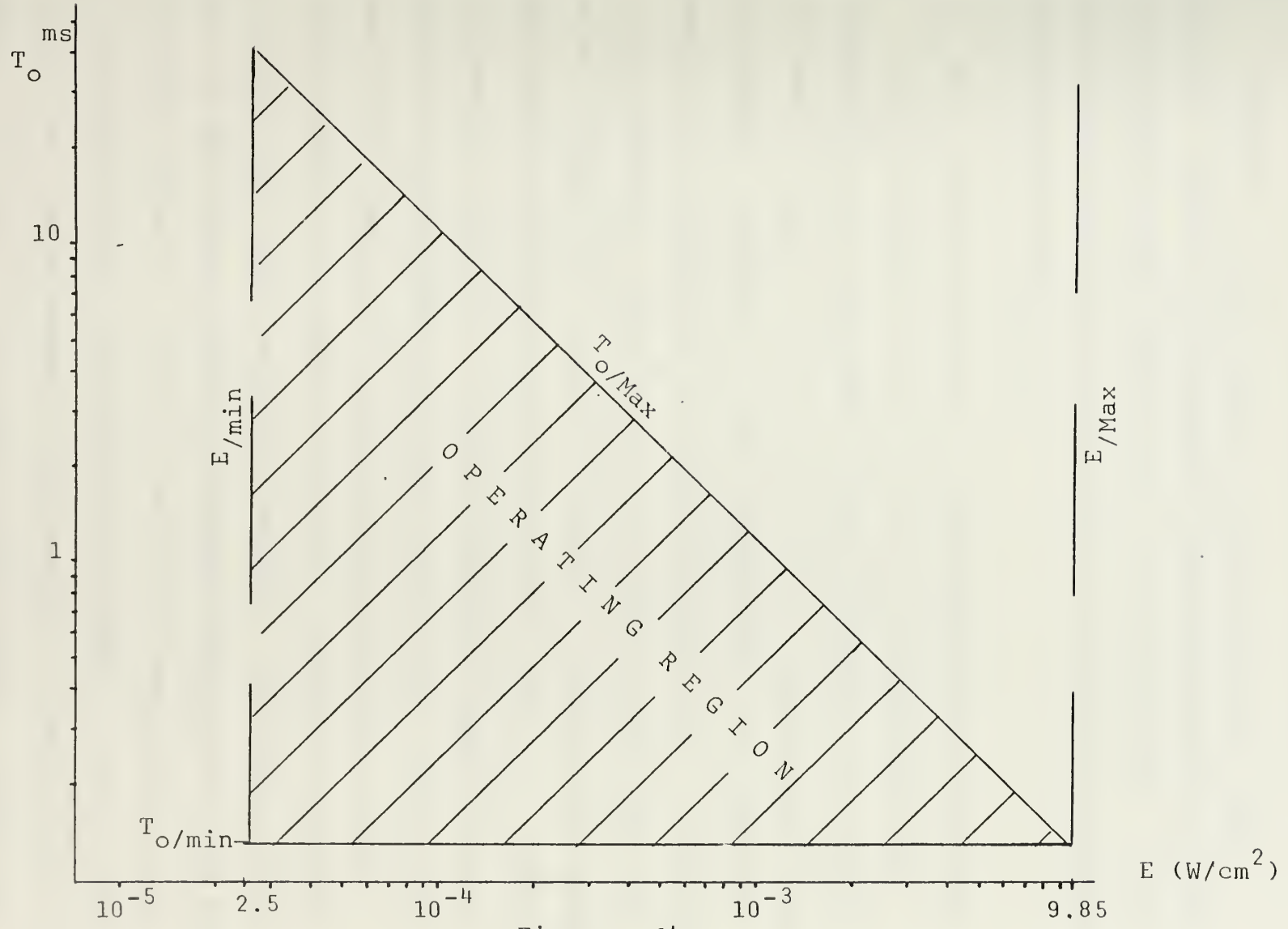
ms
T_o
10
1
$E_{/min}$
$T_{o/Max}$
OPERATING REGION
$E_{/Max}$
$T_{o/min}$
10^{-5}
2.5
10^{-4}
10^{-3}
9.85
E (W/cm^2)

Figure 24

VI. SOME APPLICATIONS OF THE DEVICE

There is a large number of applications for these devices. However as suggested by the manufacturer's sheet: "THE DEVICE IS WELL SUITED FOR O.C.R. APPLICATIONS. IT MAY BE USED FOR NON-CONTACT MEASUREMENT AND INSPECTION DEPENDING ON THE REQUIRED RESOLUTION".

A. AS A COMPUTER INTERFACE TO READ HANDWRITING CHARACTERS

Until recently the use of O.C.R. for inputting hand-printed data into computers has been limited to the reading of numerical data. With the advances and capability of this new sensor, equipment is being designed that is capable of reading the handprinted full alpha character set, in addition to the numerics. Since this is the form in which many computer transactions originate, interest in handprinting reading has steadily increased over the past few years. As a natural progression, interest in reading alphabetic handprinting is growing, and development in this area has been aided by the work of the American National Standards Institute (ANSI), which undertook the task of developing a standard for hand-printing, that could be used in general. The result of this work is the American National Standard Character Set for hand-printing, Figure 25. So big a set is not required for most of the applications, but reflects an attempt to include characters for a large number of applications. From this set the pairs S/8 and Y/V are used in this section. These are

some of the called "Troublesome Pairs". In a complete study of handwriting capability many aspects should be taken into consideration. Several techniques are being developed to overcome problems of handwriting, such as new edge detection techniques.

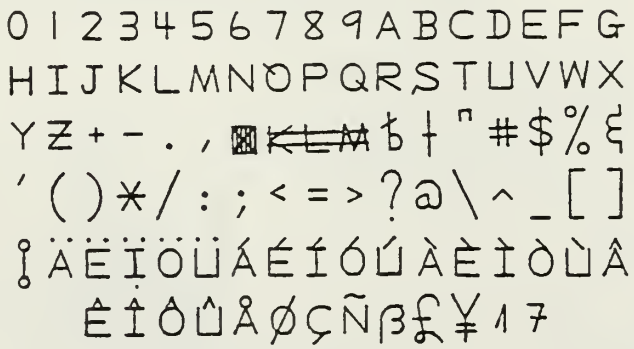

Figure 25

However for our purposes of evaluation of the array such in-depth is not necessary. An analysis based on the device resolution is presented. Using the set of Figure 25, a typical page can contain about 34 characters, that gives an approximate ratio of 4 photodiodes per letter. Figure 26 represents a schematic diagram of the set-up used in this experiment. The lenses used were from a 110 mm pocket camera. The vertical scanning provided by the rotating drum was set at the standard facsimile rate of 96 lines per inch. For our set of characters this corresponds to 20 lines per element. The image quality obtained with the system described above was very poor and no

conclusions were possible. In order to obtain some results a second experiment was done. The paper with the characters was mounted in a mobile holder, allowing to scan each letter with five lines.

For each line the output was recorded. Since the output depends on the position of the character in front of the array the process was repeated several times.

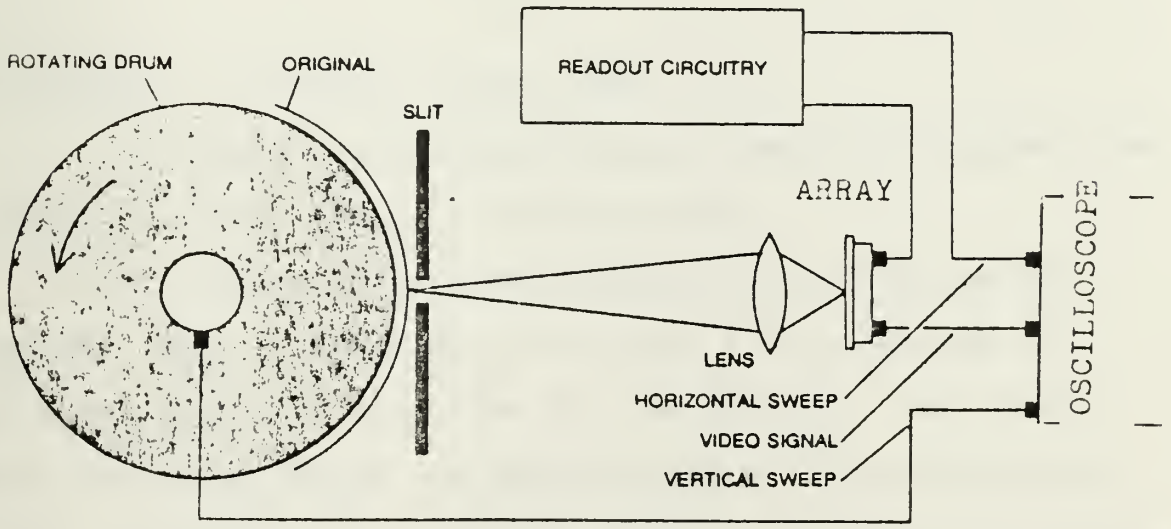

Figure 26

Figure 27 represents a summary of the results for the pair Y/V . The columns represent the average output of each photodiode, the rows the five scanning lines. The 1 and 0 represent the existence, non-existence of the output pulse, respectively. The ? represent an indetermined output, that is a value for which 1 and 0 has been obtained.

Y				V			
0	1	1	0	0	1	1	0
?	?	?	?	?	?	?	?
1	?	?	1	?	?	?	?
1	?	?	1	1	0	0	1
1	?	?	1	1	0	0	1

Figure 27

An analysis of Figure 27 shows that:

1- The first row corresponding to the first scanned line is equal for both cases, as was expected.

2- For the second row and indetermined situation was obtained, that is sometimes the output 1 was obtained for the first diode and sometimes for the second. This represents a problem, since the identification of the letter may become impossible, or misinterpretable. This analysis applies also to the remaining lines 3, 4 and 5.

As a result we can conclude that the array due to the small number of elements has a severe limitation for this application. This limitation is simply due to the resolution obtainable with the device. The experiment was repeated using the same process, but for a ratio of 8 photodiodes per character. The results are summarized in Figure 28.

Y								V							
1	0	0	0	0	0	0	1	1	0	0	0	0	0	0	1
0	?	?	0	0	?	?	0	?	?	0	0	0	0	?	?
0	0	0	?	?	0	0	0	0	?	?	0	0	?	?	0
0	0	0	?	?	0	0	0	0	0	?	?	?	?	0	0
0	0	0	?	?	0	0	0	0	0	0	?	?	0	0	0

Figure 28

As can be compared with Figure 27, Figure 28 shows a sensible improvement. As a summary the array performs well for these kinds of application, depending on the degree of resolution required.

The other conflict-pair tested was S/8 . The results are essentially the same.

B. READING THE U.P.C.

Most of the items in the supermarket now, have a series of uneven width bars showing clearly on the outside of the package or can, Figure 29.

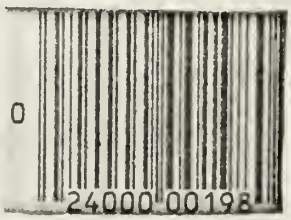

Figure 29

This is called the UNIVERSAL PRODUCT CODE (U.P.C.), and was designed to be read by a scanner, that transmits the in-

formation contained in the code to a computer. In the traditional system the operator moves the item across a window. The prices are supplied by the computer, so there is no chance of being wrongly charged by the operator. The inventory is permanently updated. Many other advantages as well as disadvantages exist. In this section we are going to apply our device to this system, with the clear advantage that the item doesn't need to be scanned mechanically, as it does in the traditional system.

The U.P.C. code has about 3.2 cm width. The thinnest black bar (or separation), is about .3 mm. Then the number of photodiodes per thin bar is:

$$\frac{128 \times .3}{32} = 1.2$$

We are practically in the limit of application of the array. Figure 30 represents the output obtained. It is a computer drawn picture of the oscilloscope display. The reason for this kind of presentation is that a clearer idea of the results is obtained, as well as an easy comparison with the input. It shows that very little coincidence exists with the input. For example, the two first thin bars are not detected, and the first large bar seems in the output to be larger than it really is.

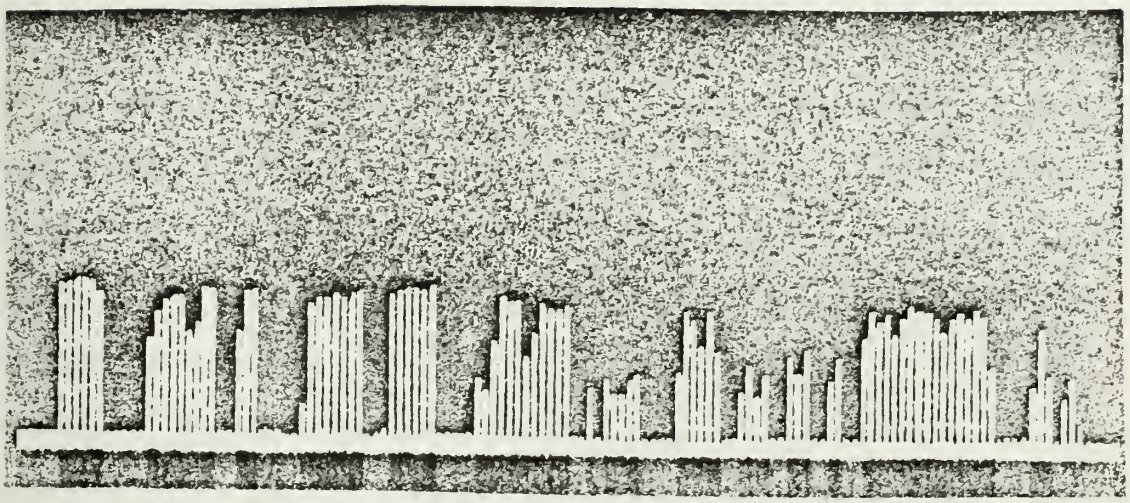

Figure 30

C. AS A SENSOR FOR A TELEVISION CAMERA TUBE

Considering the small number of elements available in the array, great results cannot be expected from the device. This experiment was set up in order to have an approximate standard television picture. A rotating mirror (galvani type), provided the mechanical scanning in one direction. Since, with the settings of the oscilloscope we can easily improve or not the image quality being received. The control of grid illumination was completely off, and the grid removed. The following sequence of pictures shows that very good results were obtained, if we take in consideration the limitations present above.

Figure 31 represents the results obtained by imaging a resolution chart with the system. The vertical and horizontal bars in the chart are not resolved by the device. This fact

was expected since we have for the entire system an approximate ratio of .47 photodiodes per mm. The largest separation between bars is about 2 mm resulting in a value of .9 photodiode per bar. It is impossible then to image correctly this portion of the chart. In the circular portion some points must be considered: In the left region of the picture we see that the radial sectors are well resolved, up to a point at which the resolution of the array, does not allow a correct reading anymore. At this point the reasoning presented above applies equally well. At the central portion of the picture we see that the resolution, is not so good. This has nothing to do with the array and must certainly be caused by reflections, causing the diodes to discharge.

Some difficulties were encountered during the performing of the experiment. For example the illumination of the target

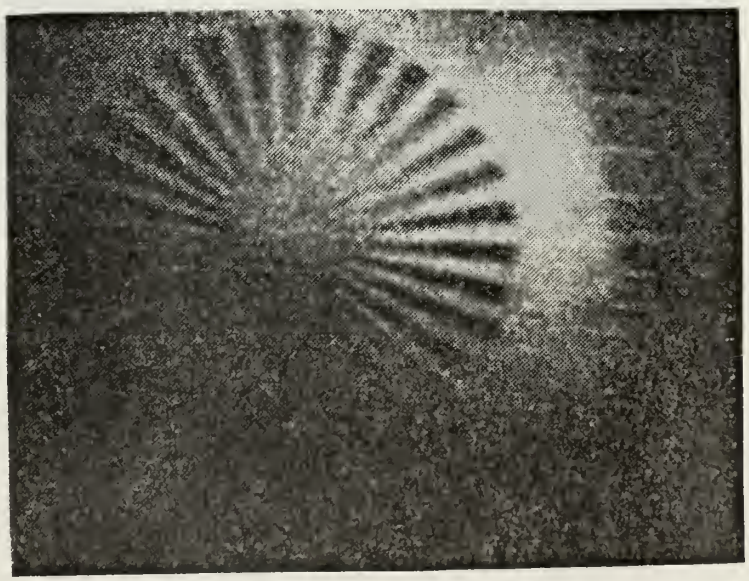

Figure 31

was rather critical. At Figure 31 a clearer region is perfectly visible. This corresponds to a saturation situation. By manually scanning it was verified that several photodiodes were well above the saturation limit. However this was necessary to get a reasonable picture. Clearly by this presents a severe limitation in the system, because there is no real output from that portion of the target. The same problem can also be verified in Figure 32. This represents the image of a page of a magazine. The considerations presented earlier apply also to this figure.

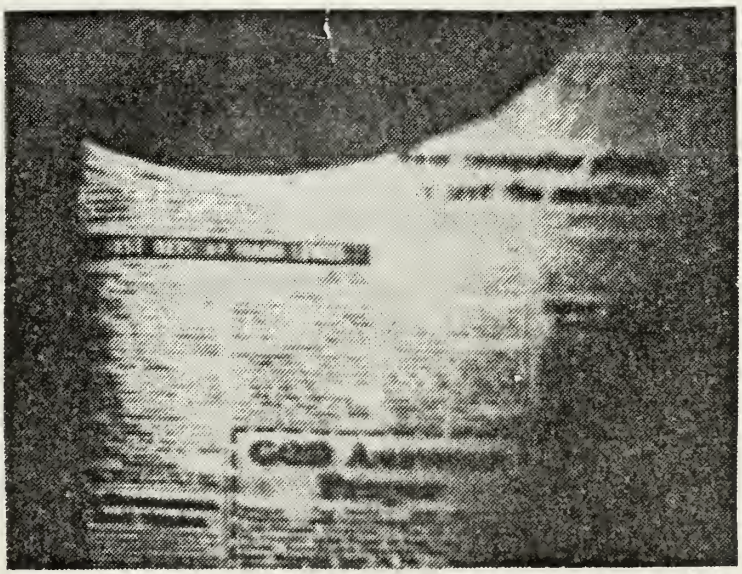

Figure 32

VII. CONCLUSION

The system described in this report is suitable for O.C.R. and facsimile display that require a small number of elements. It is also useful for small-area imaging applications where resolution need not be of television quality. In these applications, the MOS diode array is an excellent replacement for low-resolution image tubes because of its capability of operating at low light levels with self-contained power supply, and drive circuitry. The devices may be easily cascaded to provide higher resolution because the end-of-scan output is properly timed to be used as the start pulse for the next array.

The system allows a maximum sample rate of 1 Mhz. Maximum and minimum values of irradiance are 9.85×10^{-3} and 2.5×10^{-5} W/cm^2, respectively. Switching noise, that takes place in reading the array, constitutes the main limitation in the useful range of the device.

A common limitation in the applications presented in this report was the low resolution of the system. If an array with a larger number of elements were used, a sensible improvement could be expected.

LIST OF REFERENCES

1. Weckler, G. P., A silicon photodevice to operate in a photon flux integration mode, presented at the International Electron Device Meeting, Washington, DC, October 1965.

2. Biberman, Lucien M. and Nudelman, Sol, Photoelectronic Imaging Devices, Volume 2, Plenum Press, 1971.

3. Chaberlain, Savvas G., Photosensitivity and Scanning of Silicon Image Detector Arrays, IEEE Journal of Solid-State Circuits, Vol. SC-4, No. 6, December 1979.

4. Arnold, E., Crowell, M. H., Geyer, R. D., Mathur, D. P., Video Signals and Switching Transients in Capacitor-Photodiode and Capacitor-Phototransistor Image Sensors, IEEE Transactions on Electron Devices, Vol. ED-18, No. 11, November 1971.

5. Osborn, Daniel C., Sneak Paths in X-Y Matrix Arrays, IEEE Journal of Solid-State Circuits, Vol. SC-4, No. 6, December 1969.

INITIAL DISTRIBUTION LIST

		No. Copies
1.	Defense Technical Information Center Cameron Station Alexandria, VA 22314	2
2.	Library, Code 0142 Naval Postgraduate School Monterey, CA 93940	2
3.	Department Chairman, Code 61 Department of Physics and Chemistry Naval Postgraduate School Monterey, CA 93940	2
4.	Professor E. C. Crittenden, Jr., Code 61Ct Department of Physics and Chemistry Naval Postgraduate School Monterey, CA 93940	2
5.	Professor A. W. M. Cooper, Code 61Cr Department of Physics and Chemistry Naval Postgraduate School Monterey, CA 93940	1
6.	LT Carlos Jorge Guimaraes Martins Portuguese Navy Direccao do Servico de Instrucao Ministerio da Marinha Lisboa, Portugal	2
7.	Maria Margarida T.C.R. Martins Rua Frei Antonio das Chagas, 20-6^{o}Esq. Setubal, Portugal	1

Thesis 187030
M35927 Martins
c.1 Experimental study
of self-scanning
photodiode array.